

FEDSM-ICNMM2010-' 0% %

FAST INERTIAL MICROFLUIDIC ACTUATION AND MANIPULATION USING SURFACE ACOUSTIC WAVES

Leslie Y. Yeo*

James R. Friend

Micro/Nanophysics Research Laboratory
Department of Mechanical and Aerospace Engineering
Monash University
Clayton, VIC 3800, Australia
Email: leslie.yeo@eng.monash.edu.au

ABSTRACT

Though uncommon in most microfluidic systems due to the dominance of viscous and capillary stresses, it is possible to drive microscale fluid flows with considerable inertia using surface acoustic waves (SAWs), which are nanometer order amplitude electro-elastic waves that can be generated on a piezoelectric substrate. Due to the confinement of the acoustic energy to a thin localized region along the substrate surface and its subsequent leakage into the body of liquid with which the substrate comes into contact, SAWs are an extremely efficient mechanism for driving fast microfluidics. We demonstrate that it is possible to generate a variety of efficient microfluidic flows using the SAW. For example, the SAWs can be exploited to pump liquids in microchannels or to translate free droplets typically one or two orders of magnitude faster than conventional electroosmotic or electrowetting technology. In addition, it is possible to drive strong microcentrifugation for micromixing and bioparticle concentration or separation. In the latter, rich and complex colloidal pattern formation dynamics have also been observed. At large input powers, the SAW is a powerful means for the generation of jets and atomized aerosol droplets through rapid destabilization of the parent drop interface. In the former, slender liquid jets that persist up to centimeters in length can be generated without requiring nozzles or orifices. In the latter, a monodis-

persed distribution of 1–10 micron diameter aerosol droplets is obtained, which can be exploited for drug delivery and encapsulation, nanoparticle synthesis, and template-free polymer array patterning.

INTRODUCTION

Microfluidics inherently involves low Reynolds number ($Re < 1$) flows due to its small length scales that endow the system with large surface-area-to-volume ratios. As a consequence, viscous and capillary stresses are typically dominant over inertial stresses in such systems, thus rendering it considerably difficult to actuate fluids or manipulate particles in microscale devices without requiring large and cumbersome ancillary equipment such as capillary pumps. Further, the laminarity of low Reynolds number flows means that carrying out mixing in these devices is also difficult in the absence of turbulent or chaotic flows [1]. Whilst considerable advances have been made over the past decade in developing novel actuation mechanisms to carry out microscale fluid actuation and particle manipulation for a variety of microfluidic applications such as genomic and proteomic analysis, point-of-care diagnostics, drug delivery, high throughput drug screening and pathogen detection, with some technologies such as electrokinetic actuation [2] showing considerable promise, there has yet to be a reliable and robust technology that can drive microfluidics on a portable chip-based platform includ-

*Address all correspondence to this author.

ing an integrated miniature power supply. Here, we demonstrate a novel microfluidic actuation platform based on surface acoustic waves (SAWs) that has the potential to carry out such. Due to the large acoustic intensities that can generate even at low power and the rather efficient energy transfer from the actuator surface to the fluid, as will be discussed below, Reynolds numbers on the order of 10–100 are not uncommon with these technologies, and hence microscale fluid and particle motion can be induced at considerably high speeds due to the appreciable inertia that can be generated. This can also be exploited to introduce sufficient chaotic oscillation of the flow in the system to drive effective mixing. Besides fluid pumping and mixing, we also show that it is possible to use the SAW to generate a whole host of microfluidic manipulation, such as particle synthesis, concentration, sorting and patterning as well as free droplet translation, jetting, atomisation.

SURFACE ACOUSTIC WAVE MICROFLUIDICS

SAWs are electro-elastic Rayleigh waves with amplitudes on the order of 10 nm that skim the surface of a piezoelectric substrate. The SAW devices used in our work predominantly consist of a pair of interdigitated transducers (IDTs) each with several aluminum electrode finger pairs sputter-deposited onto a 127.68° yx -cut lithium niobate (LiNbO_3) piezoelectric single crystal substrate. Application of an oscillating electrical signal to the IDT using a RF signal generator and power amplifier leads to the generation of the SAW with a wavelength λ that correlates with the IDT finger width and spacing; more specifically, the finger width and spacing are both $\lambda/4$. The corresponding SAW resonant frequency is $f = c_s/\lambda$, where $c_s \approx 3965$ m/s is the speed of the SAW in the substrate.

The intricate fluid-structural coupling that arises when the SAW comes into contact with the fluid is the fundamental mechanism that gives rise to SAW microfluidics. At the leading edge of the drop (Fig. 1(A)), the SAW diffracts into the drop due to the difference between the sound velocities in the substrate c_s and the fluid, c_l (≈ 1485 m/s for water). The diffraction of the acoustic waves into the fluid occurs at a specific angle given by the ratio of the sound velocities, known as the *Rayleigh angle* $\theta_R = \sin^{-1}(c_l/c_s) \approx 22^\circ$ (Fig. 1(B)), and provides a mechanism for energy transfer into the drop. As this occurs, a longitudinal pressure wave front is generated, which drives bulk fluid recirculation within the drop, or *acoustic streaming*. The horizontal component of the energy transfer into the drop at the Rayleigh angle also results in a body force that acts on the entire drop in the SAW propagation direction, causing the drop to deform into an asymmetrical conical shape along an axis defined the Rayleigh angle (Fig. 1(C)). Eventually, the drop is driven to translate in the direction of the SAW propagation once the contact line pinning forces are exceeded.

Figure 2 shows the response of the drop to the SAW in the

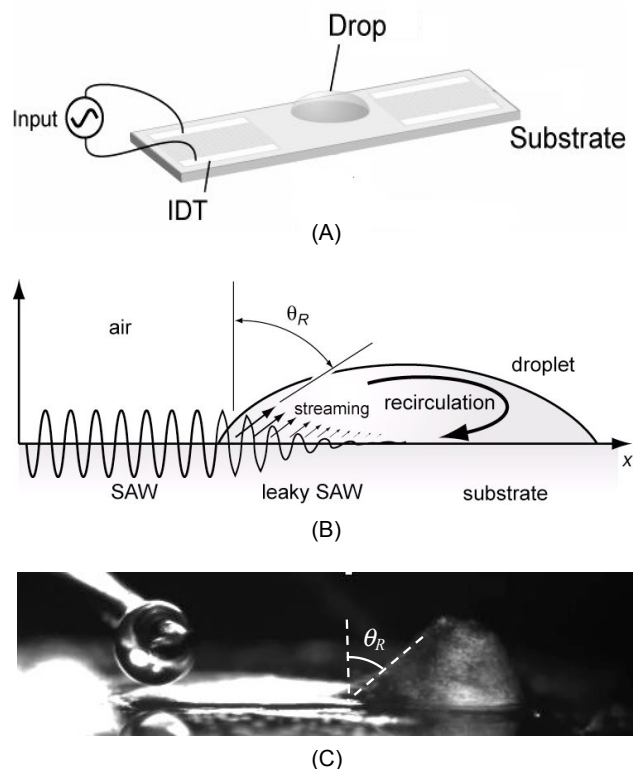


Figure 1. (A) FLUID-STRUCTURAL INTERACTION BETWEEN THE SAW AND A DROP IN ITS PROPAGATION PATHWAY CAUSES (B) THE ACOUSTIC ENERGY TO LEAK INTO THE DROP AT THE RAYLEIGH ANGLE θ_R , GIVING RISE TO ACOUSTIC STREAMING IN THE DROP AND A BODY FORCE ACTING ON THE DROP, WHICH, IN TURN, (C) CAUSES THE DROP TO DEFORM INTO AN AXISYMMETRICAL CONICAL SHAPE AND SUBSEQUENTLY TO TRANSLATE ACROSS THE SUBSTRATE.

order of increasing substrate vibration amplitude with increasing input power to the IDT [3]. At low powers, the drop deforms into the axisymmetrical conical structure shown, which also vibrates—the low amplitude capillary wave vibration here can be exploited for particle assembly and sorting on the free surface. As the input power is increased, the body force acting on the drop overcomes the contact line pinning force causing it to translate, thus allowing the SAW to be exploited for moving and manipulating drops in open microfluidic systems. If the SAW energy is concentrated underneath the drop, a peculiar jetting phenomenon occurs. Alternatively, if the vibration energy is sufficiently large to overwhelm the capillary stresses holding the drop together, drop atomization occurs. Below, we discuss each of these SAW microfluidic phenomena, as well as other manipulations that can be induced, with particular emphasis on their potential for application in practical microfluidic systems.

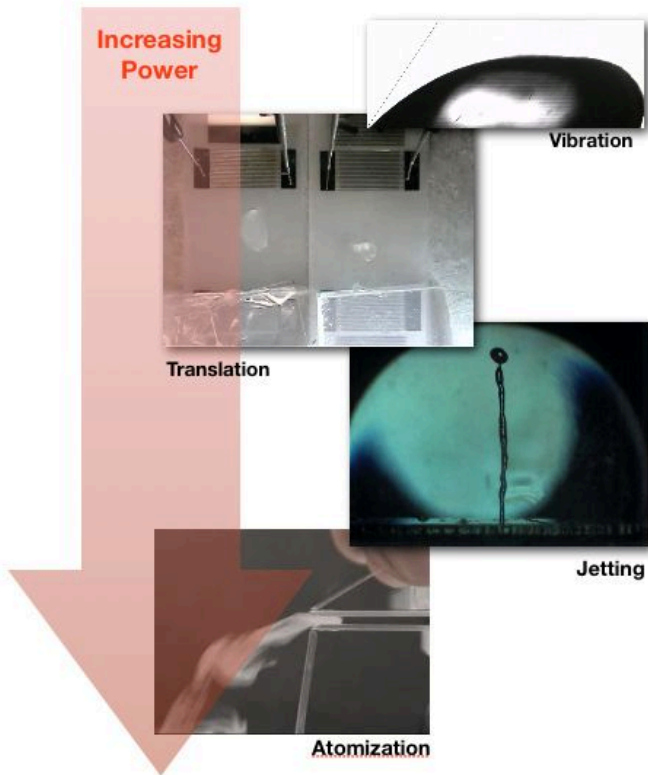


Figure 2. TYPICAL MICROSCALE FLUID MANIPULATIONS THAT CAN BE GENERATED USING THE SURFACE ACOUSTIC WAVE. IN THE ORDER OF INCREASING RF POWER APPLIED TO THE IDT: THE DROP VIBRATES, TRANSLATES (THE LEFT SHOWS A DROP TRANSLATING ON A BARE HYDROPHILIC LITHIUM NIOBATE SUBSTRATE AND THE RIGHT SHOWS THE DROP TRANSLATING ON A SUBSTRATE COATED WITH A HYDROPHOBIC LAYER), FORMS A LONG SLENDER JET, AND, EVENTUALLY ATOMIZES.

DROP VIBRATION & PARTICLE ASSEMBLY

A sessile drop containing a suspension of 500 nm particles subject to low amplitude SAW vibration gives rise to a unique particle assembly phenomenon [4]. Figure 3 shows the different particle assembly patterns that arise on the drop free surface. Initially, the colloidal particles assemble into linear concentric rings coinciding with the nodal lines of the low amplitude 20 MHz standing wave vibrations induced on the free surface, as shown by the fingerprint-like patterns in Regime A. As the SAW vibration is increased, the colloidal particles in the linear ringlike assemblies are observed to cluster to form pointwise colloidal islands as depicted by the patterns in Regime B. This regime is associated with large amplitude 1 kHz order vibrations associated with the capillary-viscous resonance of the drop. The colloidal islands therefore appear to form at the intersection between the nodal lines of the low amplitude 20 MHz standing wave vibration and the circular nodal ring of the large amplitude 1 kHz capillary-

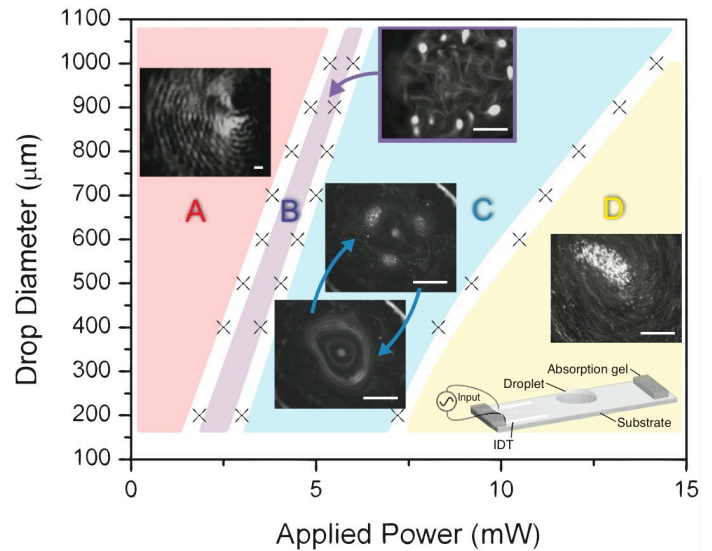


Figure 3. FREE SURFACE COLLOIDAL PATTERNS AS A FUNCTION OF THE INITIAL DROP DIAMETER AND INPUT POWER [4]. THE SCALE BARS CORRESPOND TO 200 MICRON LENGTH SCALES.

viscous vibration of the drop. Further increases in the SAW vibration amplitude leads to the onset of significant fluid streaming within the drop which disperses the particles and hence erases the colloidal island assemblies (Regime C). The streaming, however, only lasts for a short transient before ceasing, at which point the colloidal islands are observed to reform until the streaming recommences and erases them again. This cyclic phenomenon occurs aperiodically and the direction of the streaming (clockwise and anticlockwise) is noted to be reasonably random, suggesting that this regime is a transient metastable state and that the commencement and cessation of the streaming is triggered by a peculiar instability arising from the highly nonlinear coupling between the acoustic, hydrodynamic and capillary forces. With further increases in the SAW vibration, however, the streaming becomes stronger and more consistent, leading to permanent dispersion of the particles (Regime D).

DROP TRANSLATION & MICROCHANNEL PUMPING

If the SAW vibration amplitude is sufficiently large such that the body force imparted by the leakage of the SAW irradiation on a sessile drop sitting on the substrate overcomes the surface forces that pin the contact line of the drop, the drop can be linearly translated at speeds typically around 1–10 cm/s [5,6], which are one to two orders of magnitude larger than the speeds that can be achieved through other actuation schemes, for example, electrowetting [7]. This drop translation capability has been employed for various biological applications, e.g., transport of DNA in discrete droplets for polymerase chain reaction [8], rapid bioparticle collection and concentration for biosensing ap-

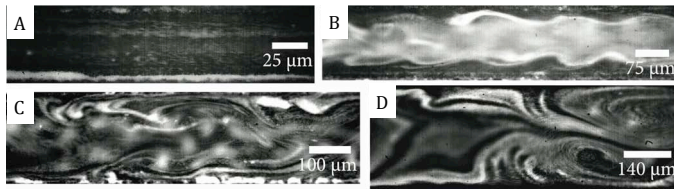


Figure 4. FLOW STRUCTURE AS A FUNCTION OF THE MICROCHANNEL WIDTH W FOR A FIXED OPERATING FREQUENCY. AS W IS INCREASED, IT CAN BE SEEN THAT THE UNIFORM THROUGH FLOW FOR FLUID PUMPING IN (A) IS PROGRESSIVELY REPLACED BY AN OSCILLATORY CHAOTIC FLOW AS SEEN IN (B)–(D), WHICH CAN BE EXPLOITED FOR CONCURRENT FLUID MIXING IN THE SAME DEVICE [13].

plications [6] and efficient seeding of cells into bioscaffolds for tissue and orthopedic engineering [9, 10]. Due to the high frequency associated with the SAW, the cells are not observed to be denatured; their differentiation and proliferation capabilities also appear to remain intact [11].

In addition, the SAW can be used to pump liquid through microchannels [12, 13]. As with the SAW-driven drop transport, the micropumping velocities achieved are extremely high, on the order 1 cm/s, which is one to two decades larger than that possible with electrokinetic micropumps [14]. Due to the transmission of sound waves into the fluid through the undulating channel walls as the SAW traverses, it is also possible to switch between uniform through flow for fluid delivery, as shown in Fig. 4(a), and chaotic oscillatory flow for micromixing, as shown in Figs. 4(b)–4(d) [13]. This can be achieved either by altering the microchannel width keeping the SAW excitation frequency constant, as shown in Fig. 4, or by changing the SAW frequency for a fixed width microchannel.

If, on the other hand, the fluid contained a suspension of colloidal particles and the input power is below the threshold required for fluid flow, the particles are observed to collect in a linear particle assembly along the nodes of the pressure field corresponding with the first order fluid motion arising due to the compressibility of the sound waves that are radiated into the fluid. The number of nodal lines and the number of aligned particle assemblies can be seen to correlate closely, as seen in Fig. 5. Such particle manipulation behavior can then be exploited for microchannel particle focusing [15].

MICROCENTRIFUGATION

It is possible to generate microcentrifugation by symmetry breaking of the SAW through a number of ways, as shown in Fig. 6 [16]. The azimuthal fluid recirculation can be further intensified by pointwise focusing the SAW beneath the drop with the use of the curved electric-width-controlled single-phase unidirectional transducer (SPUDT) electrodes shown in Fig. 7(A)

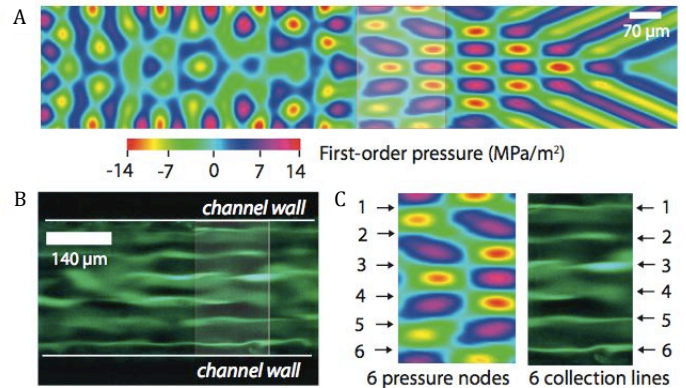


Figure 5. COMPARISON BETWEEN (A) THE COMPUTED FIRST ORDER PRESSURE FIELD IN THE FLUID AND (B) THE NUMBER OF LINEAR 500 NANOMETER COLLOIDAL PARTICLE ASSEMBLIES THAT ARISE IN THE QUIESCENT FLUID REGION. IT CAN BE SEEN IN (C) THAT THE PARTICLES APPEAR TO COLLECT ALONG THE NODAL LINES OF THE PRESSURE FIELD [13].

in place of the conventional IDT design [17, 18]. Unlike the conventional bidirectional IDT design shown schematically in Fig. 1(A), internally tuned reflectors within the IDT fingers in the SPUDT electrode design generates a unidirectional SAW that propagates from a single side of the IDT. The corresponding SAW pattern, which can be visualized through laser Doppler vibrometry (LDV) or simply through the patterns arising from the deposition of smoke particles, as shown in Figs. 7(B) and 7(C), respectively. Recirculatory flows in the azimuthal direction with linear velocities of around 1 mm/s with the conventional IDTs and as high as 20 mm/s with the focusing SPUDTs are observed, which can be exploited to drive intense micromixing. Shilton *et al.* [18] have shown that the chaoticlike inertial flow generated provides a means for driving effective turbulent-like mixing with an enhancement ratio D_{eff}/D_0 that scales roughly as the square of the input power, where D_{eff} is the effective diffusivity and D_0 is the diffusivity in the absence of flow. In [18], a small amount of food dye is shown to be completely mixed in a glycerine-water drop in under 1 sec. We have shown this intense mixing to be extremely useful for microscale chemical and biochemical synthesis—yields comparable or even significantly higher than that obtained using ultrasound or microwave chemistry have been demonstrated with significantly shorter reaction times [19]. In addition, rapid particle concentration and separation can also be achieved if the drop is suspended with micro- or nano-particles, as shown in Fig. 8, in which the particles are seen to concentrate in under 1 s, thus providing a convenient and effective means for pathogen preconcentration for fast and sensitive detection in biosensors or the separation of red blood cells from plasma in miniaturized point-of-care diagnostic kits.

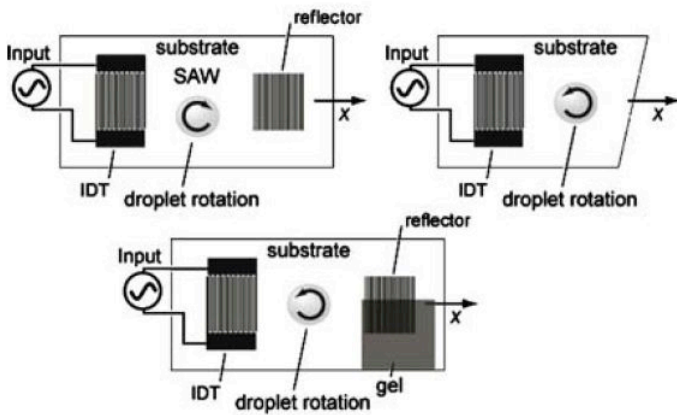


Figure 6. MICROCENTRIFUGATION WITHIN A SESSILE DROP CAN BE GENERATED THROUGH SYMMETRY BREAKING OF THE SAW RADIATION ACROSS THE SUBSTRATE EITHER BY PLACING THE DROP OFF-CENTER (TOP-LEFT), THROUGH ASYMMETRIC REFLECTION OF THE SAW BY INTRODUCING A DIAGONAL CUT AT THE EDGE OF THE SUBSTRATE (TOP-RIGHT) OR THROUGH THE USE OF ABSORPTION GEL TO SUPPRESS THE REFLECTION AT ONE-HALF OF THE IDT (BOTTOM) [16].

JETTING & ATOMIZATION

Finally, if the input power and hence the SAW vibration intensity is sufficiently large such that the capillary stresses maintaining the shape of the parent drop is overcome, resulting in significant interfacial deformation. At these high powers, the substrate displacement velocity as the SAW traverses along the substrate surface is typically 1 m/s irrespective of the excitation frequency. Given the SAW substrate vibration amplitude of approximately 10 nm, large surface accelerations, on the order of 10 million g 's can typically be generated, which in turn, drives the interfacial destabilization. If the SAW energy is concentrated to a point underneath the drop with the use of two elliptical focusing SPUDTs at two opposite ends, the transmission of radiation at the Rayleigh angle into the liquid from both the front and rear of the drop causes it to deform into a coherent elongated liquid column, as shown in Fig. 9 [20]. It is therefore possible to generate a fluid jet that persists over centimeters in length from a millimeter diameter drop without requiring fluid confinement mechanisms such as nozzles or orifices to accelerate the fluid to adequately sufficient velocities necessary to produce an elongated jet. Not only does this demonstrate the ability for the SAW to drive strong inertial forcing on a liquid, the ability to induce such jets could have potential applications in inkjet or soft biological printing, fiber synthesis, and drug delivery, amongst others. Figure 10 shows the rich dynamics of the jetting phenomenon, in which we observe the jet length and the ability to generate single or multiple droplet ejection to depend on the jet Weber number $We_j \equiv \rho U_j^2 R_j / \gamma$, where ρ is the fluid density, U_j the jet velocity, R_j the jet radius and γ the interfacial tension.

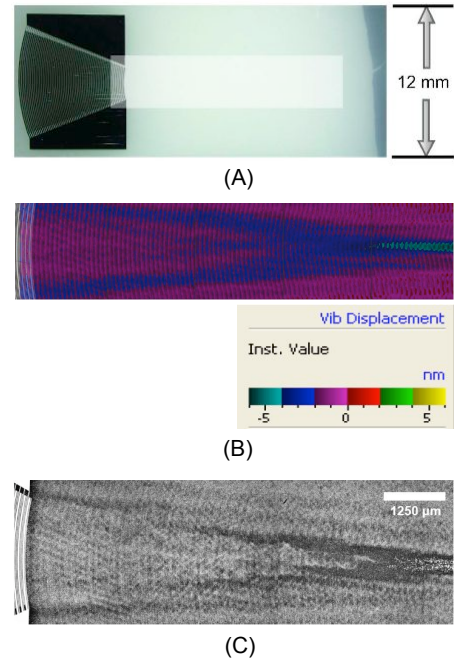


Figure 7. (A) FOCUSING ELLIPTICAL SPUDT. THE CORRESPONDING SAW PATTERNS THAT ARE GENERATED, OBTAINED USING (B) LDV, AND, (C) SMOKE PARTICLE DEPOSITION, INDICATE THE INTENSIFICATION OF THE SAW TOWARDS A FOCAL POINT [17, 18].

If the power is not focused to a point underneath the drop or if the input power to the IDTs is further increased, the entire drop is completely destabilized and atomizes to produce aerosol droplets with a monodisperse distribution around a mean diameter 5 μm [21]. These monodispersed micron-sized aerosol droplets are particularly useful as drug-carrying vehicles for pulmonary drug delivery in which 2–5 μm droplet sizes are typically required for optimum dose efficiency in order to deliver the maximum amount of drug to the lower respiratory airways for direct local administration to target organs [22]. The power required, typically 1 W or less, is at least a factor of ten smaller than that of ultrasonic atomizers which use Langevin transducers and single lead zirconium titanate element thickness-mode piston atomizers operating between 10 kHz and 1 MHz. At these lower frequencies, drug molecules, DNA or proteins are susceptible to denaturing as cavitation becomes prevalent. Indeed, we demonstrate that the post-atomization biomolecular viability and function is preserved [23]. Another advantage of the SAW atomization technique, as with the jetting phenomenon discussed above, is the ability to do away with nozzles and orifices which are prone to clogging, thus simplifying considerably the device and hence reducing its costs and increasing its reliability.

By atomizing a polymer solution, it is also possible to produce 150–200 nm spherical clusters of polymeric nanoparticles comprising sub-50 nm particulates, as shown in the schematic in Fig. 11 [24]. This one-step process for nanoparticle synthesis is

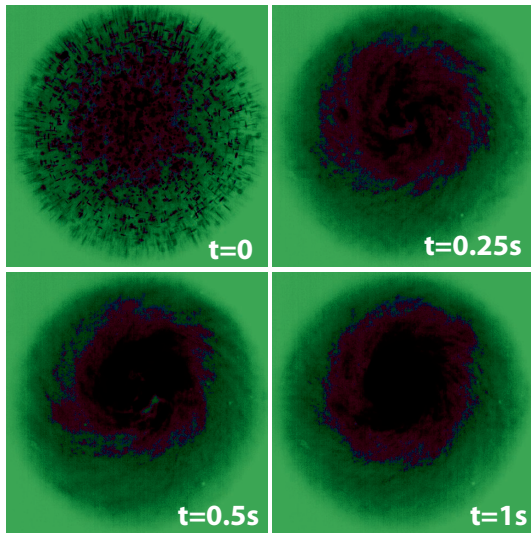


Figure 8. CONCENTRATION OF 500 NANOMETER FLUORESCENT PARTICLES IN A 0.5 MICROLITER WATER DROP DUE TO THE INERTIAL BULK FLUID RECIRCULATION THAT DRIVES STRONG MICRO-CENTRIFUGATION WITHIN THE DROP [18].

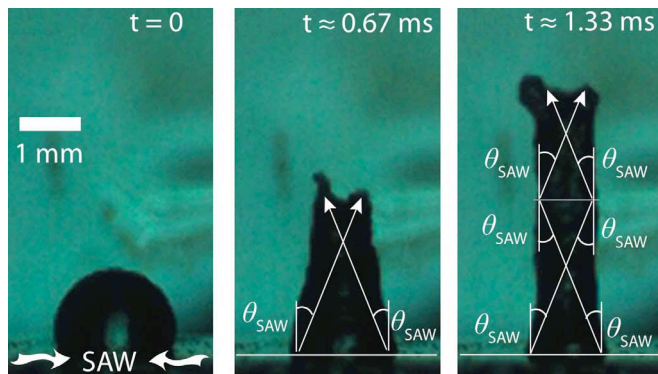


Figure 9. ELONGATED JET GENERATED BY CONCENTRATING THE SAW INTO THE DROP [20].

therefore a straightforward, fast and attractive alternative to the multistep conventional methods for nanoparticle production such as spray drying, nanoprecipitation, emulsion photocross-linking, etc., which are slow and cumbersome. In addition, we have also demonstrated the possibility of generating 100 nm order dimension protein (insulin) nanoparticles as well as 3 µm aerosol droplets for inhalation therapy [25]. Further, it is possible to load protein and other therapeutic molecules into the biodegradable polymer nanoparticle shells produced for controlled release drug delivery [26]. The encapsulation of the drug within the biodegradable polymer essentially shields the drug from rapid hydrolysis and degradation, permitting sustained release over time, and thus prolonging the effect of the drug over longer periods whilst preventing dangerous dose spikes. Our recent inves-

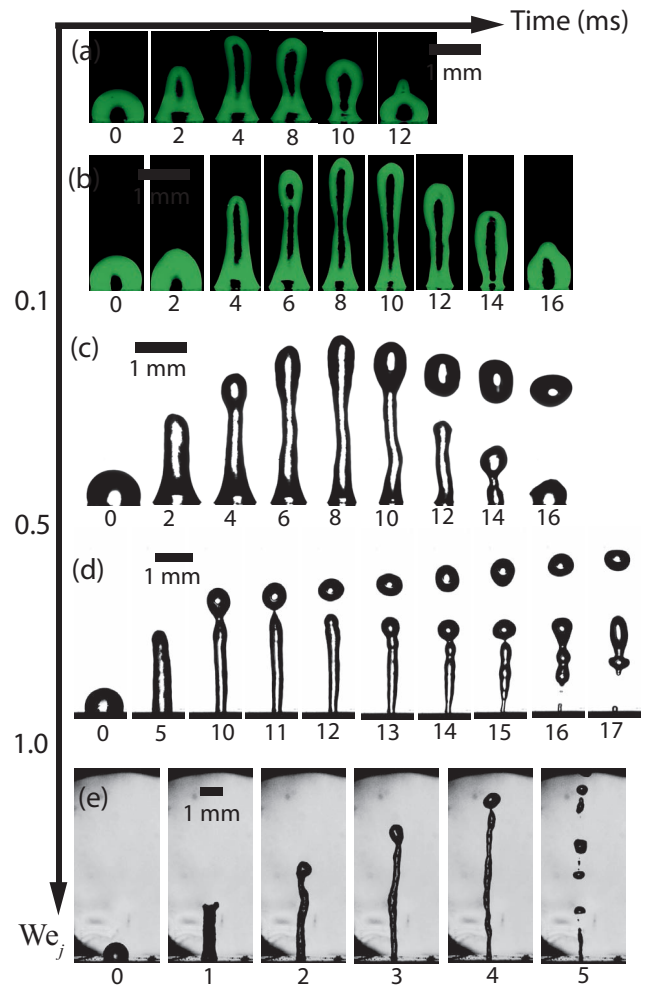


Figure 10. SAW JETTING AS A FUNCTION OF TIME, SHOWING THE DEPENDENCE OF ITS LENGTH AND BREAK-UP ON THE JET WEBER NUMBER We_j [20].

tigations have indicated the viability of primary mammalian osteoblast stem cells after SAW atomization thus suggesting that the technique can be used for drug loading without altering the nature of the biomolecule [11].

SAW atomization also offers the potential for the long-range, regular spatial-ordering of polymer spot patterns on a substrate without physical or chemical templating or other surface treatment procedures [27]. As shown in Figs. 12(a) and 12(b), the translation of a drop containing the polymer solution leaves behind a thin trailing film, which simultaneously destabilizes, thus thinning the film at the antinodes of the standing SAW vibration and resulting in its depletion of the film there. The breakup of the film across the entire substrate surface at these positions and the subsequent evaporation of the solvent then yields the evenly spaced solidified polymer droplet patterns shown in Figs. 12(c) and 13(a). The pattern periodicity as well as

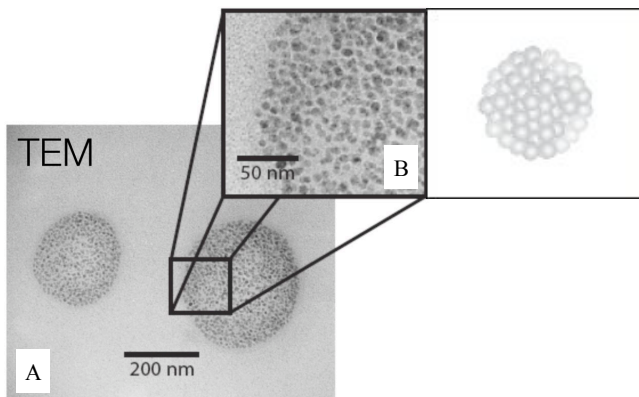


Figure 11. SYNTHESIS OF POLYMER NANOPARTICLES AROUND 150–200 NANOMETER IN DIAMETER WITH SURFACE ACOUSTIC WAVE ATOMIZATION. (A) TRANSMISSION ELECTRON MICROSCOPY (TEM) IMAGE OF A NANOPARTICLE. (B) MAGNIFICATION OF THE IMAGE SHOWING THE AGGREGATION OF SUB-50 NANOMETER PARTICULATES TO FORM A 200 NANOMETER CLUSTER, THE SCHEMATIC SHOWING A RECONSTRUCTION OF THE PARTICLE AGGREGATE [24].

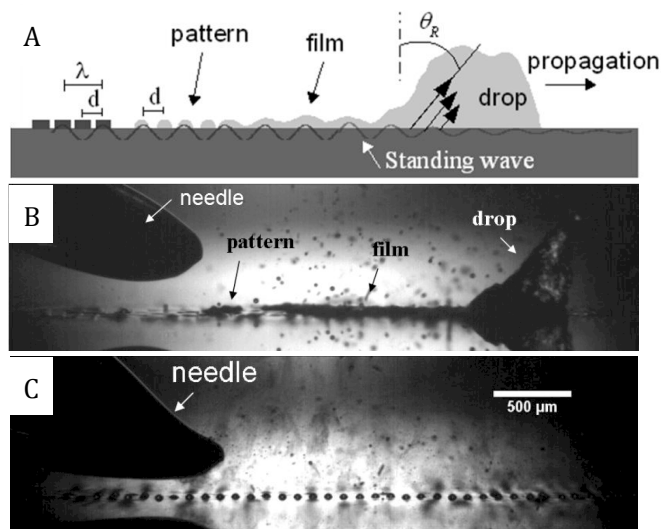


Figure 12. LONG-RANGE REGULAR POLYMER SPOT PATTERNING ARISING FROM THE ATOMIZATION OF A THIN FILM OF POLYMER SOLUTION DISPENSED FROM THE NEEDLE ABOVE THE SUBSTRATE (A,B). THE INITIAL DROP THAT IS DISPENSED TRANSLATES IN THE DIRECTION OF THE SAW PROPAGATION, LEAVING BEHIND A THIN TRAILING FILM, WHICH SUBSEQUENTLY DESTABILIZES AND ATOMIZES, THUS LEAVING BEHIND (C) SOLIDIFIED POLYMER SPOTS AT THE ANTINODAL POSITIONS [27].

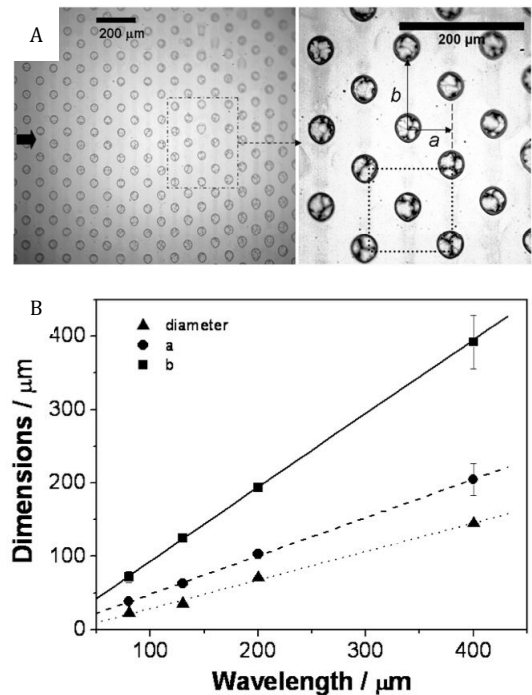


Figure 13. (A) POLYMER SPOT PATTERNING. (B) SPOT DIAMETER, LONGITUDINAL PITCH SPACING A AND TRANSVERSE PITCH SPACING B AS A FUNCTION OF THE SAW FREQUENCY AND WAVELENGTH [27].

the polymer spot size is observed to strongly correlate with the SAW frequency or wavelength, as shown in Fig. 13(b), therefore presenting the ability for control and fine tuning, which is a key advantage over other conventional patterning methods [27].

ACKNOWLEDGMENT

This work would not have been possible without close collaboration with J. Friend and the talented students and postdocs who have shared in our journey on SAW microfluidics and whose work has led to the discoveries described above. They are, in alphabetical order, M. Alvarez, D. Arifin, K. Kulkarni, H. Li, A. Qi, R. Shilton, R. Raghavan and M. K. Tan. In addition, we would also like to thank our collaborators A. Dasvarma (Australian Stem Cell Centre), M. P. McIntosh (Monash University), A. Mechler (LaTrobe University), D. A. Morton (Monash University), P. Perlmutter (Monash University), L. Spiccia (Monash University) and K. Traianedes (Australian Stem Cell Centre). We also acknowledge funding from the Australian Research Council (Discovery Projects DP098525 & DP1092955; Linkage, Infrastructure, Equipment & Facilities LP0668435), the National Health and Medical Research Council (Development Grant 1000513), Nanotechnology Victoria, and the Research Support for Counter-Terrorism programme administered by the

REFERENCES

- [1] Stone, H. A., Stroock, A. D., and Adjari, A., 2004. "Engineering Flows in Small Devices: Microfluidics Toward a Lab-on-a-Chip". *Annual Review of Fluid Mechanics*, **36**, pp. 381–411.
- [2] Chang, H.-C. and Yeo, L. Y., 2010. *Electrokinetically Driven Microfluidics and Nanofluidics* (Cambridge, New York).
- [3] Yeo, L. Y. and Friend, J. R., 2009. "Ultrafast Microfluidics Using Surface Acoustic Waves". *Biomicrofluidics*, **3**, 012002.
- [4] Li, H., Friend, J. R., and Yeo, L. Y., 2008. "Microfluidic Colloidal Island Formation and Erasure Induced by Surface Acoustic Wave Radiation". *Physical Review Letters*, **101**, 084502.
- [5] Renaudin, A., Tabourier, P., Zhang, V., Camart, J. C., and Druon, C., 2006. "SAW Nanopump for Handling Droplets in View of Biological Applications". *Sensors and Actuators B*, **133**, pp. 389–397.
- [6] Tan, M. K., Friend, J. R., and Yeo, L. Y., 2007. "Microparticle Collection and Concentration Via a Miniature Surface Acoustic Wave Device". *Lab on a Chip*, **7**, pp. 618–625.
- [7] Yeo, L. Y. and Chang, H.-C., 2005. "Static and Spontaneous Electrowetting". *Modern Physics Letters B*, **19**, pp. 549–569.
- [8] Guttenberg, Z., Müller, H., Habermüller, H., Geisbauer, A., Pipper, J., Falbel, J., Kielpinski, M., Scriba, J., and Wixforth, A., 2005. "Planar Chip Device for PCR and Hybridization with Surface Acoustic Wave Pump". *Lab on a Chip*, **5**, pp. 308–317.
- [9] Li, H., Friend, J. R., and Yeo, L. Y., 2007. "A Scaffold Cell Seeding Method Driven by Surface Acoustic Waves". *Biomaterials*, **28**, pp. 4098–4104.
- [10] Bok, M., Li, H., Yeo, L. Y., and Friend, J. R., 2009. "The Dynamics of Surface Acoustic Wave-Driven Scaffold Cell Seeding". *Biotechnology and Bioengineering*, **103**, pp. 387–401.
- [11] Li, H., Friend, J., Yeo, L., Dasvarma, A., and Traianedes, K., 2009. "Effect of Surface Acoustic Waves on the Viability, Proliferation and Differentiation of Primary Osteoblast-like Cells". *Biomicrofluidics*, **3**, 034102.
- [12] Girardo, S., Cecchini, M., Beltram, F., Cingolani, R., and Pisignano, D., 2008. "Polydimethylsiloxane–LiNbO₃ Surface Acoustic Wave Micropump Devices for Fluid Control Into Microchannels". *Lab on a Chip*, **8**, pp. 1557–1563.
- [13] Tan, M. K., Yeo, L. Y., and Friend, J. R., 2009. "Rapid Fluid Flow and Mixing Induced in Microchannels Using Surface Acoustic Waves". *Europhysics Letters*, to appear.
- [14] Laser, D. J. and Santiago, J. G. , 2004. "A Review of Micropumps". *Journal of Micromechanics and Microengineering*, **14**, pp. R35–R64.
- [15] Shi, J., Mao, X., Ahmed, D., Colletti, A., and Huang, T. J., 2008. "Focusing Microparticles in a Microfluidic Channel With Standing Surface Acoustic Waves (SSAW)". *Lab on a Chip*, **8**, pp. 221–223.
- [16] Li, H., Friend, J. R., and Yeo, L. Y., 2007. "Surface Acoustic Wave Concentration of Particle and Bioparticle Suspensions". *Biomedical Microdevices* **9**, pp. 647–656.
- [17] Tan, M. K., Friend, J. R., and Yeo, L. Y., 2007. "Direct Visualization of Surface Acoustic Waves Along Substrates Using Smoke Particles". *Applied Physics Letters*, **91**, 224101.
- [18] Shilton, R., Tan, M. K., Yeo, L. Y., and Friend, J. R., 2008. "Particle Concentration and Mixing in Microdrops Driven by Focused Surface Acoustic Waves". *Journal Applied Physics*, **104**, 014910.
- [19] Kulkarni, K., Friend, J., Yeo, L., and Perlmutter, P., 2009. "Surface Acoustic Waves as an Energy Source for Drop Scale Synthetic Chemistry". *Lab on a Chip*, **9**, 754–755.
- [20] Tan, M. K., Friend, J. R., and Yeo, L. Y., 2009. "Interfacial Jetting Phenomena Induced by Focused Surface Vibrations". *Physical Review Letters*, **103**, 024501.
- [21] Qi, A., Yeo, L. Y., and Friend, J. R., 2008. "Interfacial Destabilization and Atomization Driven by Surface Acoustic Waves". *Physics of Fluids*, **20**, 074103.
- [22] Qi, A., Friend, J. R., Yeo, L. Y., Morton, D. A. V., McIntosh, M. P., and Spiccia, L., 2009. "Miniature Inhalation Therapy Platform Using Surface Acoustic Wave Microfluidic Atomization". *Lab on a Chip*, **9**, pp. 2184–2193.
- [23] Qi, A., Yeo, L., Friend, J., and Ho, J., 2010. "The Extraction of Liquid, Protein Molecules and Yeast Cells From Paper Through Surface Acoustic Wave Atomization". *Lab on a Chip*, **10**, pp. 470–476.
- [24] Friend, J. R., Yeo, L. Y., Arifin, D. R., and Mechler, A., 2008. "Evaporative Self-Assembly Assisted Synthesis of Polymeric Nanoparticles By Surface Acoustic Wave Atomization". *Nanotechnology*, **19**, 145301.
- [25] Alvarez, M., Friend, J. R., and Yeo, L. Y., 2008. "Rapid Generation of Protein Aerosols and Nanoparticles Via Surface Acoustic Wave Atomization". *Nanotechnology*, **19**, 455103.
- [26] Alvarez, M., Yeo, L. Y., and Friend, J. R., 2009. "Rapid Production of Protein-Loaded Biodegradable Microparticles Using Surface Acoustic Waves". *Biomicrofluidics*, **3**, 014102.
- [27] Alvarez, M., Friend, J. R., and Yeo, L. Y., "Surface Vibration Induced Spatial Ordering of Periodic Polymer Patterns on a Substrate". *Langmuir*, **24**, pp. 10629–10632.